



HAL
open science

Spectral analysis and structural response of periodic and quasi-periodic beams

Safiullah Timorian, Giovanni Petrone, Sergio de Rosa, Francesco Franco, Morvan Ouisse, Nouredine Bouhaddi

► **To cite this version:**

Safiullah Timorian, Giovanni Petrone, Sergio de Rosa, Francesco Franco, Morvan Ouisse, et al.. Spectral analysis and structural response of periodic and quasi-periodic beams. Proceedings of the Institution of Mechanical Engineers, Part C: Journal of Mechanical Engineering Science, 2019, 233 (23-24), pp.7498-7512. <10.1177/095440621988894>. <hal-02402880>

HAL Id: hal-02402880

<https://hal.science/hal-02402880v1>

Submitted on 10 Dec 2019

HAL is a multi-disciplinary open access archive for the deposit and dissemination of scientific research documents, whether they are published or not. The documents may come from teaching and research institutions in France or abroad, or from public or private research centers.

L'archive ouverte pluridisciplinaire **HAL**, est destinée au dépôt et à la diffusion de documents scientifiques de niveau recherche, publiés ou non, émanant des établissements d'enseignement et de recherche français ou étrangers, des laboratoires publics ou privés.



HAL Authorization

Spectral analysis and structural response of periodic and quasi-periodic beams

S. Timorian^{1,2}, G. Petrone¹, S. De Rosa¹, F. Franco¹, M. Ouisse²,
and N. Bouhaddi²

¹PASTA Lab —Laboratory for Promoting experience in
Aeronautics Structures, Department of Industrial Engineering -
Aerospace Section, University of Naples Federico II, Napoli, via
Claudio 21, 80125, Italy.

²Univ. Bourgogne Franche-Comté, Femto-ST Institute,
Department of Applied Mechanics, Besancon, 25000, France.

Abstract

Periodic structures found a big interest in engineering applications because they introduce frequency band effects, due to the impedance mismatch generated by periodic discontinuities in the geometry, material or boundary conditions, that can improve the vibroacoustic performances. However, the presence of defects or irregularity in the structure, leads to a partial lost of regular periodicity (called *quasi-periodic structure*) that can have a noticeable impact on the vibrational and/or acoustic behaviour of the elastic structure. The irregularity can be tailored to have impact on dynamical behaviour. In the present paper numerical studies on the vibrational analysis of one-dimensional finite, periodic and quasi-periodic structures are presented. The contents deal with the finite element models of beams focused on the spectral analysis and the damped forced responses. The quasi-periodicity is defined by invoking the Fibonacci sequence for building the assigned variations (geometry and material) along the span of finite element model. Similarly, the same span is used as a super unit cell with Floquet-Bloch conditions waves for analysing the infinite periodic systems. Considering both longitudinal and flexural elastic waves, the frequency ranges corresponding to band gaps are investigated. The wave characteristics in quasi-periodic beams, present some elements of novelty and could be considered for designing structural filters and controlling the properties of elastic waves.

1 Introduction

The analysis of the propagation of waves in structures is a fundamental task in many engineering applications. The knowledge of dispersion relations, pro-

viding information on the type and nature of propagating waves is of interest for the prediction of forced response, acoustic radiation, non-destructive testing and transmission of structure-borne sound. All these themes are nowadays the subject of many studies in order to improve the vibro-acoustic comfort of passenger carries, bridges, pipelines, and space vehicles.

Wave propagation in simple structures can be investigated through analytical models, exact or approximated. However, this kind of analysis usually involves assumptions and approximations concerning the stress, strain and displacement states of the structure, and always more refined numerical models are required as the frequency increases since the wavelength may become comparable with the cross-section dimensions. For example, if the propagation of bending waves in a beam is investigated, Euler-Bernoulli, Rayleigh, Timoshenko or 3-dimensional elasticity-based theories might be used, depending on the frequency range of interest [1, 2]. For complex structures, such as layered (composite and sandwich) beam [3, 4, 5] and plate [6, 7, 8, 9, 10, 11, 12], or cylinders [13, 14, 15], analytical formulations become quite difficult: beyond the required assumptions and approximations in the models, the resulting dispersion relations are usually transcendental and/or of high order, therefore their resolution is not straightforward or requires symbolic manipulation [15, 16]. For this reason, for the analysis of complex structural components, semi-analytical or numerical methods have been developed for the computation of dispersion curves. However, if the structure under investigation presents characteristics which are periodically repeated in one or more directions, the analysis procedure can take advantage of this property by exploiting the periodicity [17]. A generic structure obtained as an assembly of identical elements, called cells, can be considered as periodic. Several engineering structures can be assumed as periodic, starting from simple beams and plates, moving to stiffened plates or car tyres, up to aircraft fuselages, railways, tracks, etc. In this case the study of the wave propagation through the waveguide can be reduced to the analysis of a single cell by applying the periodicity conditions together with continuity of displacements and equilibrium of forces at the interfaces between two consecutive cells (Floquet-Bloch theorem) [18, 19, 20].

Periodic structures found a big interest in engineering applications because they introduce frequency band effects that can improve the vibroacoustic performances. In fact, in periodic structures, the impedance mismatch generated by periodic discontinuities in the geometry, acting as a waveguide, and/or in the material, can cause destructive wave interference phenomena over specific frequency bands called “stop band“ or “band gaps“ [21]. However, the presence of imperfections (i.e. defects or irregularity) in the structure, due to the manufacturing process or not exact reconstructions of the boundary conditions for example, lead to the loss of the periodicity of the structure: this can have a noticeable impact on the vibrational and/or acoustic behaviour of the elastic structure.

In this case it is more correct to speak about quasi-periodicity which is the

property of a structure that displays irregular periodicity. A quasi-periodic structure can be idealised as repeated substructures which have asymmetric translations in any direction of the Euclidian space. It can be considered as an intermediate case between periodic and random elastic medium [22]. Quasi-periodic behaviour is thus a pattern of recurrence with a component of unpredictability that does not lend itself to a precise measurement. An example of a natural quasi-periodic structure is a quasicrystal. It was discovered in 1981 by Dan Shechtman [23, 24] and it is a structural form that are both ordered and non-periodic [16]. These structures are characterized by several properties, such as low coefficient of friction and low heat conductivity, just to cite some of them, that made them very attractive and interesting for technological applications, mainly in the fields of crystallography and photonics [23, 24, 25, 26, 27, 28, 29]. Quasi-crystals were used as non-stick coating on frying pans and cooking utensils [30] and to develop heat insulation, led and new materials able to convert heat to electricity [31, 32, 33].

In recent years there is a growing interest in the design possibilities offered by quasi-periodic structures also in the field of structural mechanics. This leads to some modelling issues which will be well analysed due to the impossibility of periodic simplifications, but an adequate design of the quasi-periodicity may offer new vibroacoustic properties to the structure [34, 38, 39, 40], they also provide experimental verification of the transmission properties of one dimensional phononic crystals based on the quasi-periodic Fibonacci and Thue-Morse number sequence. Hou et al. [34] investigated the transmission properties and the frequency spectra of Fibonacci binary composite material with different thickness ratio of two layers. Whereas in this paper Fibonacci series is dedicated for $1D$ structures i.e. beams and the vibration properties and band structure of their unit cells are investigated. In term of analysis this paper is mainly focused on Frequency Response Functions (FRF) and spectral analysis to study the dynamic behaviour of the structures [35, 36, 37]. Aynaou et al. [38] performed a theoretical investigation on acoustic wave propagation of one-dimensional phononic band gap structures made of slender tube loops pasted together with slender tubes of finite length according to a Fibonacci sequence. In this analysis Aynaou et al, found that besides the existence of extended and forbidden modes, some narrow frequency bands appear in the transmission spectra inside the gaps as defect modes. Similarly, in the results of the current investigation, there are narrow frequency peaks that appears in the frequency bands of the geometrical impedance mismatch case, especially on longitudinal frequency response. Aynaou et al consists a treatment procedure that spatial localisation of the modes lying in the middle of the bands and at their edges is examined by means of local density of states. In the other hand, Chen and Wang [39] studied band gaps of elastic waves propagating in one-dimensional disordered phononic crystals. Similar topological formation of Fibonacci and Thue-Morse are investigated in an experimental observation of the formation of phononic scattering band structure in one-dimensional periodically and quasi-periodically based on the Fibonacci and Thue-Morse number sequences by King and Cox [40]. Gei [41] shows that in the case of axial and flexural vibration for

systems based on different Fibonacci sequences, the number of stop/pass bands within a defined range of frequencies changes and follows the Fibonacci recursion rule, by showing also a self-similar pattern. From a design point of view the asymmetrical conditions in quasi-periodic structures can be built by following different sequences, such as: higher order generations of Fibonacci sequence, Thue-Morse, Rudin Shapiro sequences as well as Penrose lattices [42]. In this paper the modelling of simple quasi-periodic structures is built with the conventional finite element method (FEM) to fulfil the generation of quasi-periodic patterns since these are based on an asymmetrical distribution of identical cells [43, 44]. Finite, periodic and quasi-periodic structures are thus proposed and compared by using the Fibonacci sequence to investigate about the possibility to have and control useful frequency bands in which the response can be reduced as much as possible. In Section 2 the models and their specific lexicon are presented. Section 3 contains the methods and tools used for the numerical investigations. The main results obtained are commented in Section 4 and finally, some concluding remarks are given in Section 5.

2 Models and Lexicon

In this paper, quasi-periodic beams with a finite number of cells are analysed. In these models specific sequences like Fibonacci series will be used to generate impedance mismatches in view of the desired degree of quasi-periodicity [45, 46]. The degree of quasi-periodicity might be controlled with mathematical rules that will be introduced in the next section.

2.1 Fibonacci Sequence and Nomenclature

The well-known sequence called Fibonacci [49] is a series of integer numbers such that:

$$S_n = S_{n-1} + S_{n-2} \quad (1)$$

For instance the Fibonacci sequence starting with 1 and 2 is 1, 2, 3, 5, 8, 13, 21,....The configuration of the quasi-periodic structures is here carried out by using a sequence of two possible variations according to Fig.1.

The variations can typically be due to the sections, materials or boundary conditions. The first cell coincides with S_1 , then the cells can be assembled, forming a sequence defined by a simple integer (order). The S_n denote the n -th sequence:

Tab.1 shows the number of unit cells necessary to generate a given order of Fibonacci sequence.

The numerical models is identified by the order of the Fibonacci sequence, and thus the length of the n -th order sequence, S_n , will be greater than S_{n-1} . As example, Fig.2 shows a Fibonacci (S_6) beam with a sequence of 13 [ABAABABAABAAB] cross-sections.

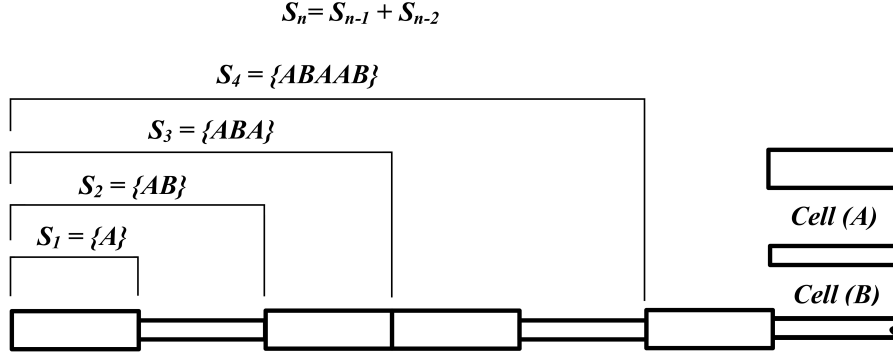


Figure 1: Configurations of quasi-periodic beam following a Fibonacci pattern[22].

Table 1: Example of number of cells according to Fibonacci orders.

Fibonacci orders function of number of cells								
Orders	4 th	5 th	6 th	7 th	8 th	9 th	10 th	11 th
Number of Cells	5	8	13	21	34	55	89	144

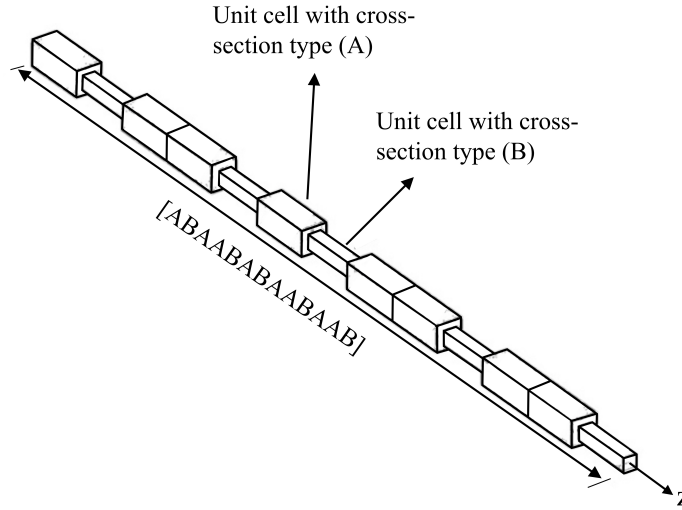


Figure 2: Fibonacci configuration of 6th order

2.2 Cases

In this framework, variations between cells A and B will be obtained through impedance mismatch. Two cases will be considered.

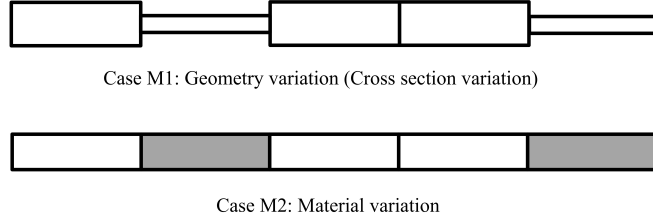


Figure 3: Configuration of discontinuities: (M1) and (M2).

Case M1: impedance mismatch due to geometrical discontinuity, Fig.3 [case M1];

Case M2: impedance mismatch due to material discontinuity, Fig.3 [case M2].

The various configurations considered for M1 will be described in the next section. Without loss of generality, the material used in case M1 is steel A-36 whose properties are provided in Tab.2

For the typical quasi-periodic structure case M2 the material variation is reported in Tab.2.

Table 2: Mechanical properties of quasi-periodic bi-material beam.

Material	Modulus of elasticity (Pa)	Poissons Ratio	Density ($\text{kg} \cdot \text{m}^{-3}$)
Steel A-36	2×10^{11}	0.26	7800
Aluminium 2045-T4	73×10^9	0.33	2700
Magnesium	45×10^9	0.35	1770
Copper	110×10^9	0.355	8960

2.3 Geometrical variations of case M1

A comparison for the case M1 by keeping constant the mass of the sum of the A and B cells is considered. The aim is to find the most efficient geometrical variation behaviour of unit cells (A) and (B) for vibration control. The factors prescribed in Tab.3 are the ratio of the length of section edges. The four configuration types are displayed in Fig.4. The configuration Type IV has no impedance mismatch, and Type II will be first analysed as a reference.

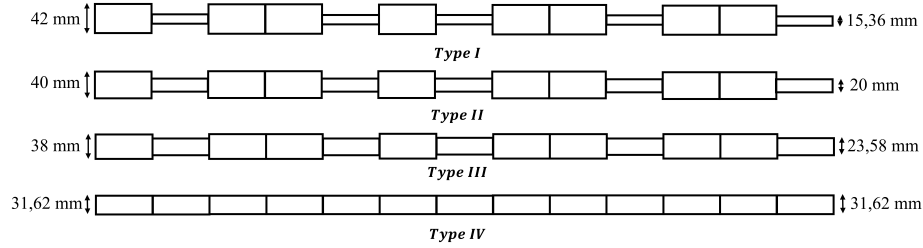


Figure 4: Comparison of case M1 by keeping constant the mass and the length of sum of the A and B cells (the beams have square cross sections).

Table 3: Sizes of cells A and B as sub-cases for M1.

Geometrical variation				
Type	Cell	width [mm]	height [mm]	Factor
I	A	42.00	42.00	2.7
	B	15.36	15.36	
II	A	40.00	40.00	2
	B	20.00	20.00	
III	A	38.00	38.00	1.6
	B	23.58	23.58	
IV	A	31.62	31.62	1
	B	31.62	31.62	

3 Methods and Tools

Two numerical methods are used: the FEM is considered for analysing the Frequency Response Functions (FRF) of the finite beam while the Wave Finite Element Method (WFEM) together with spectral analysis is taken into account for computing the dispersion diagrams.

3.1 Finite Element Analysis

The analysis is performed with the conventional FE method: frequency response function (FRF) analysis of damped quasi-periodic beams. The FE analysis is carried out using ANSYS-APDL linked with MATLAB.

The types of elements used are Beam 188, which is a linear 2-node beam element. Each cell (A and B) are composed of 4 nodes (three beam elements) and each node has three degrees of freedom: longitudinal in the axial direction (x axis), bending in lateral direction (y axis), and torsional rotation around (x axis). The actual distance between each cell is 100 mm.

$$H_{kj}(\Omega) = \sum_{p=1}^N \frac{\psi_{pk}\psi_{pj}}{m_p(\omega_p^2 - \Omega^2 + i2\xi_p\omega_p\Omega)} \quad (2)$$

where $H_{kj}(\Omega)$ is the transfer function, m_p the modal mass, ω_p the eigenfrequency, Ω the forcing frequency; ξ_p is the modal damping; ψ_{pk} and ψ_{pj} are the components of the p -th eigenvector evaluated at the source and receiver points and N the number of retained eigenmodes. Accordingly, the FRF of the quasi-periodic beams are computed.

These forced response analysis are performed with free-free boundary conditions. The input force is located at one end of the beam in the transverse direction and the response is computed at the other end of the beam in the same direction.

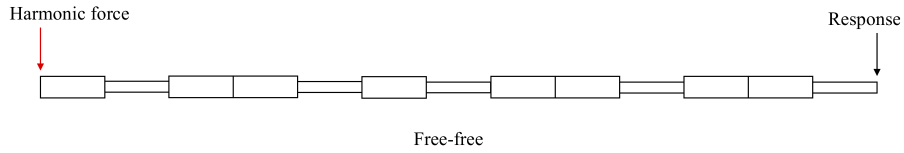


Figure 5: Schematic diagram of beam with 6th order of Fibonacci for numerical analysis.

3.2 Spectral analysis of infinite beam (waveguide)

The Floquet-Bloch conditions can be applied to simulate infinite periodic beams that is waveguides. This is classical for perfectly periodic structures. In order to perform spectral analysis on quasi-periodic structures, super unit cells are used.

3.2.1 Super unit cell:

In this work, a super unit cell is a cell hosting every single order of the Fibonacci sequence and it hosts given orders of deterministic quasi-periodic pattern in a single cell. Although it will be repeated in a periodic way, the cell itself has a quasi-periodicity replication inside the super unit cell. In this work, we also consider a second case, called double unit cell, as a reference. This case is perfectly periodic. For illustration, the substructures in Fig.6 and Fig.7 are modelled as a super unit cell and double cell respectively. In this example, the super unit cell is defined according to the 6th order of Fibonacci sequence (type ABAABABAABAAB). The super unit cell is used in the Wave Finite Element Method (WFEM) analysis presented in the next section.

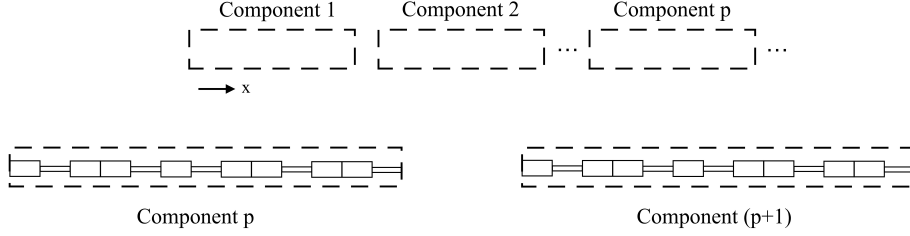


Figure 6: Periodic wave-guide (Super unit cell with 6th order of the Fibonacci sequence).

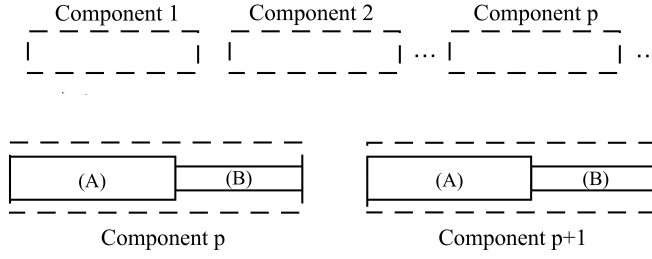


Figure 7: Periodic wave-guide (reference double unit cell).

3.2.2 Transfer matrix of super unit cell:

The transfer matrix is a square matrix of even dimension and is function of frequency of the disturbance propagating in the structure [52]. For a given structure, each super unit cell composed of n individual cells, has the same transfer matrix $[\mathbf{T}]$ such that;

$$\mathbf{x}_n = \mathbf{T}\mathbf{x}_0 \quad (3)$$

where \mathbf{x}_n is the state vector on the left-side of the cell (i.e. on the left-side of the super unit cell), \mathbf{x}_0 is the state vector on the right-side of cell 1 (i.e. on the right-side of the super unit cell), and $\mathbf{T} = \mathbf{T}_n\mathbf{T}_{n-1}, \dots, \mathbf{T}_1$ where \mathbf{T}_j is the transfer matrix of cell j . In order to obtain the transfer matrices, both mass and stiffness matrices are extracted from APDL-ANSYS.

The dynamic behaviour of the cell number j is described by:

$$\mathbf{D}^j \mathbf{q}^j = \mathbf{f}^j \quad (4)$$

where $\mathbf{D}^j, \mathbf{f}^j$, and \mathbf{q}^j define respectively the dynamic stiffness matrix, force and displacement vector. The dynamic stiffness matrix writes

$$\mathbf{D}^j = -\omega^2 \mathbf{M}^j + \mathbf{K}^{j*} \quad (5)$$

with $\mathbf{K}^{j*} = \mathbf{K}^{j*}(1 + i\eta)$ where $\mathbf{M}^j, \mathbf{K}^j$, and η are respectively the mass matrix, the stiffness matrix and the loss factor corresponding to the structural damping. The matrices and vectors are partitioned according to the degrees of freedom: \mathbf{q}_L^j , \mathbf{q}_I^j , and \mathbf{q}_R^j respectively refer to the left-side, internal, and right-side parts of the super unit cell number j . The corresponding terms in the matrices are written

$$\begin{bmatrix} \mathbf{D}_{LL}^j & \mathbf{D}_{LI}^j & \mathbf{D}_{LR}^j \\ \mathbf{D}_{LI}^{jT} & \mathbf{D}_{II}^j & \mathbf{D}_{IR}^j \\ \mathbf{D}_{LR}^{jT} & \mathbf{D}_{IR}^{jT} & \mathbf{D}_{RR}^j \end{bmatrix} \begin{Bmatrix} \mathbf{q}_L^j \\ \mathbf{q}_I^j \\ \mathbf{q}_R^j \end{Bmatrix} = \begin{Bmatrix} \mathbf{f}_L^j \\ \mathbf{0} \\ \mathbf{f}_R^j \end{Bmatrix}. \quad (6)$$

The internal degrees of freedom can then be condensed using the second row of Eq.6, in order to retain the analysis to the left and right boundary displacements and forces.

$$\mathbf{q}_I^j = -\mathbf{D}_{II}^{j-1} (\mathbf{D}_{LI}^{jT} \mathbf{q}_L^j + \mathbf{D}_{IR}^j \mathbf{q}_R^j). \quad (7)$$

it leads to

$$\begin{bmatrix} \mathbf{D}_{LL}^j - \mathbf{D}_{LI}^j \mathbf{D}_{II}^{j-1} \mathbf{D}_{IL}^j & \mathbf{D}_{LR}^j - \mathbf{D}_{LI}^j \mathbf{D}_{II}^{j-1} \mathbf{D}_{IR}^j \\ \mathbf{D}_{RL}^j - \mathbf{D}_{RI}^j \mathbf{D}_{II}^{j-1} \mathbf{D}_{IL}^j & \mathbf{D}_{RR}^j - \mathbf{D}_{RI}^j \mathbf{D}_{II}^{j-1} \mathbf{D}_{IR}^j \end{bmatrix} \begin{Bmatrix} \mathbf{q}_L^j \\ \mathbf{q}_R^j \end{Bmatrix} = \begin{Bmatrix} \mathbf{f}_L^j \\ \mathbf{f}_R^j \end{Bmatrix}. \quad (8)$$

The reduced dynamic stiffness matrix is written as follow:

$$\begin{bmatrix} \tilde{\mathbf{D}}_{LL}^j & \tilde{\mathbf{D}}_{LR}^j \\ \tilde{\mathbf{D}}_{LR}^{jT} & \tilde{\mathbf{D}}_{RR}^j \end{bmatrix} \begin{Bmatrix} \mathbf{q}_L^j \\ \mathbf{q}_R^j \end{Bmatrix} = \begin{Bmatrix} \mathbf{f}_L^j \\ \mathbf{f}_R^j \end{Bmatrix}. \quad (9)$$

One define state vectors for the boundaries of the component j :

$$\mathbf{u}_L^j = \begin{Bmatrix} \mathbf{q}_L^j \\ \mathbf{f}_L^j \end{Bmatrix}, \mathbf{u}_R^j = \begin{Bmatrix} \mathbf{q}_R^j \\ \mathbf{f}_R^j \end{Bmatrix}. \quad (10)$$

The transfer matrix is hence obtained by reorganising the degrees of freedom according to the state vector:

$$\mathbf{u}_R^j = \mathbf{T}^j \mathbf{u}_L^j \quad (11)$$

where, \mathbf{u}_L^j and \mathbf{u}_R^j are the displacement vector of the right and left component of the unit cell, and \mathbf{T}^j is the transfer matrix in Eq.11:

$$\mathbf{T}^j = \begin{bmatrix} -\tilde{\mathbf{D}}_{LR}^{j-1} \tilde{\mathbf{D}}_{LL}^j & -\tilde{\mathbf{D}}_{LR}^{j-1} \\ \tilde{\mathbf{D}}_{RL}^j - \tilde{\mathbf{D}}_{RR}^j \tilde{\mathbf{D}}_{LR}^{j-1} & \tilde{\mathbf{D}}_{LL}^j \tilde{\mathbf{D}}_{RR}^j \tilde{\mathbf{D}}_{LR}^{j-1} \end{bmatrix}. \quad (12)$$

The transfer matrix of the super unit cell is then obtained in Eq.3.

3.2.3 Dispersion analysis:

Periodicity conditions applied on the super unit cells are then written as

$$\mathbf{u}_L^{p+1} = e^\mu \mathbf{u}_L^p \quad (13)$$

where μ is the propagation constant. Combining Eq.11 and Eq.13,yields to the eigenvalue problem:

$$\mathbf{T}^p \phi_i = \lambda \phi_i. \quad (14)$$

where $\lambda = e^\mu$.

Depending on the nature of the eigenvalue of $[\mathbf{T}^p]$, the waves propagating in a periodic structure are described as travelling waves and attenuating waves which occur in alternating frequency bands known as pass-bands and stop-bands. If the eigenvalues of $[\mathbf{T}^p]$ are complex and of the form $e^{\pm ikL}$, $k \in \mathbb{R}$ the corresponding wave is in a pass-band and the wave travels in the form of $e^{\pm ikL}$, where k is a real wave number, the positive and negative signs indicating left and right travelling waves, respectively. On the other hand if all eigenvalue of the $[\mathbf{T}^p]$ are of the form $e^{\pm\beta}$ or $e^{\pm\beta+i\pi}$, $\beta \in \mathbb{R}$, is pure real exponent, the corresponding frequency is in a stop-band and the wave amplitude after travelling n elements are attenuated by the factor $e^{(\pm\beta n)}$, in which the real exponent β implies attenuated waves [52].The dispersion curves are computed by imposing frequency and computing k according to the given eigenvalue problem.

4 Frequency response function of finite beams using FEM

FRFs of finite structures are analysed in two subsections according to the cases named M1 and M2.

The FRFs are plotted in wider frequency ranges of 10 kHz for flexural and 25 kHz for axial vibration. The frequency range was chosen for the first 22 natural frequencies. A modal analysis is taken into consideration to investigate the number of elements per wavelength in order to fulfil a criterion for a sufficiently accurate numerical modal analysis. The boundary condition is free-free and a frequency range up to 10kHz for flexural and 25 kHz for axial vibration is chosen because the main target is on the first 22 natural frequencies. The model is meshed by 1D 2-node beam element type 188. Mesh setting with two different beam elements (188 – 2 node and 189 – 3 node) with the number of elements per wavelength 4, 5, and 10 are checked. The span of the beam is 1300 mm and 39 elements per wave length was more accurate with beam element 188 – 2 node to converge the exact natural frequency which is 9700 Hz.

The strategy to compute the harmonic response function of periodic beams is carried out in MATLAB. A script is created to define finite element model of the periodic double cell with an arrangement of 13 unit cells. The boundary condition is considered as free-free and a white noise (i.e. harmonic force of $1N$

from 0 – 10 kHz with a bandwidth of 10 Hz is applied to one end of the beam. The white noise is applied in vertical z and horizontal x direction, respectively for flexural and longitudinal vibrations.

4.1 FRF results for Case M1-Type II

A first analysis of M1-Type II is performed, considering increasing orders of the Fibonacci sequence (4^{th} , 5^{th} , 6^{th} , 7^{th} , 8^{th} , 9^{th} , 10^{th} , and 11^{th} orders). It is reminded that the structure is not periodic, and that an increase in Fibonacci order is associated to an increase in the length of the beam. All results are carried out in the frequency range [0 – 10000] Hz. The results in Fig.8 shows multiple stop bands which stay coherent from one order to the other, for instance, around [600 – 900] Hz, [1900 – 2300] Hz and a larger frequency stop band around [2900 – 4000] Hz.

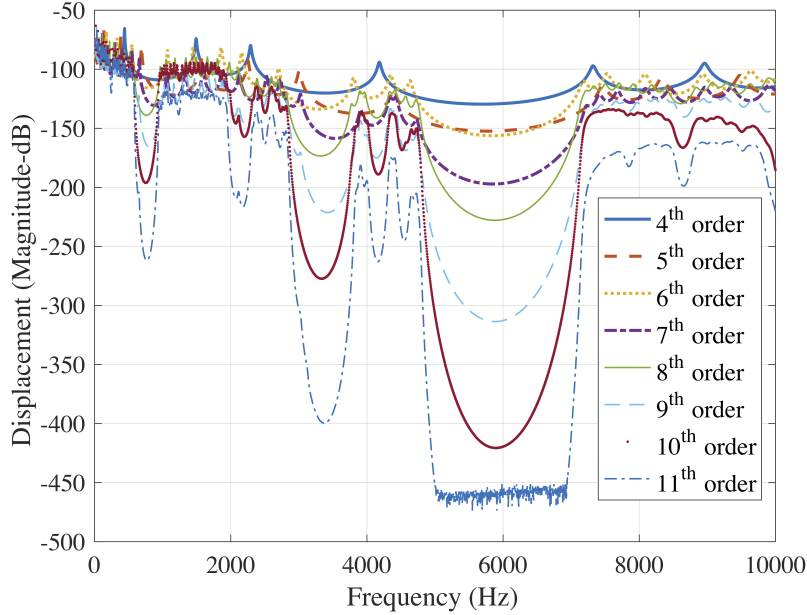


Figure 8: FRFs of the flexural waves for given orders of Fibonacci beam with geometrical variation

The trend is similar to periodic structures when the number of cells increases: the band gaps location does not change, while the depth in the FRF is becoming larger. The largest frequency stop band appears around [4900 – 7100] Hz. The

lowest depth of the amplitude that exceeds (-450) decibels corresponds to the precision of the numerical tool and is obviously not measurable in practice. The dark blue curve corresponds to the highest generated order of Fibonacci, the 11^{th} order in this investigation and shows the deepest gaps. Other curves follow in unequal increment in the depth as the generation order is increasing. The picks which can be observed in the Fig.8 corresponds to the resonances of the finite beams.

Beside the flexural response shown in Fig.8, a similar analysis is performed for the longitudinal waves. Fig.9 shows responses of the beams with an applied force in the axial direction. There are only two stop bands around $[4300 - 4800]$ Hz and $[6600 - 10000]$ Hz.

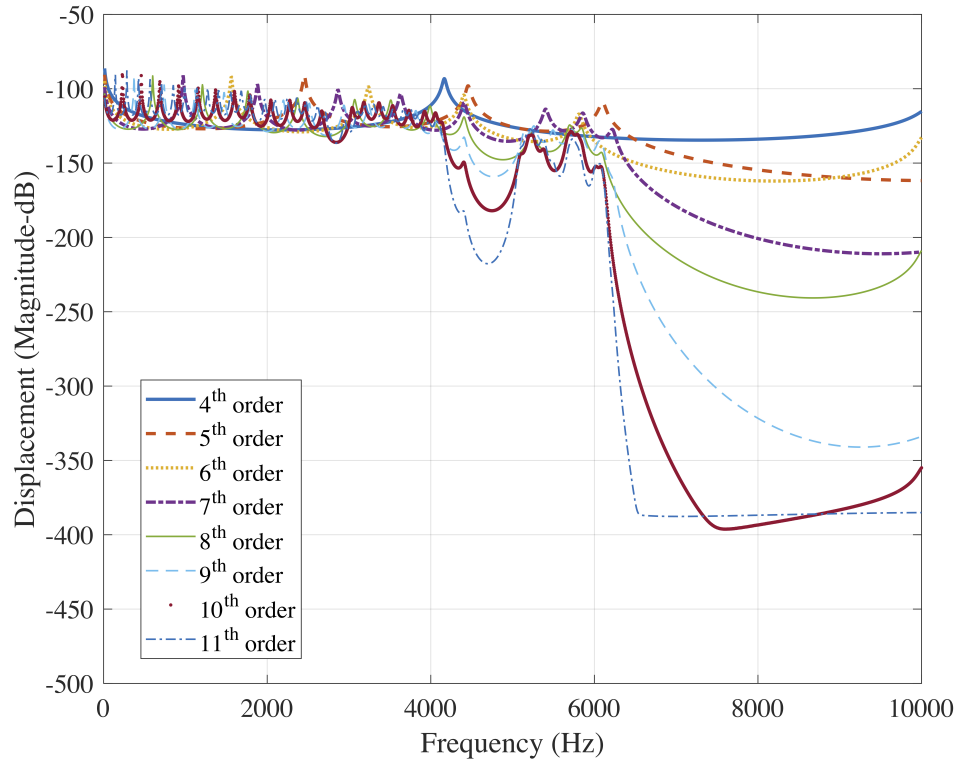


Figure 9: FRFs of the longitudinal waves for given orders of Fibonacci beam with geometrical variation

The trend is similar to the flexural waves shown in Fig.8 when the number of cells is increasing: the band gaps locations do not change, while the depth in the FRF is becoming larger. There is also a localised mode which is appearing inside the band gap of longitudinal waves. The effects of dynamic behaviour of the beam-spans when increasing the number of cells following Fibonacci orders

is emphasised by this analysis. In practice, these types of beam-spans can be used as a junction filter between structures. The induced vibrational energy transfers through this junction, and it acts as a meta-material filtering property to the elastic waves due to the impedance mismatch in geometry and material.

4.2 Frequency response function of double cell and super unit cell structure using WFEM:

In this part, FRFs of periodic beams are analysed. Two cases are considered, a double cell variation with a span of 13 unit cells having perfect periodic order and a super unit cell Fibonacci 6th order with 13 unit cells, which has non-symmetric repetition of cells inside periodic super unit cell. The results are discussed with four types of variations in geometry for both cases. The aim of this analysis is to investigate the effect of the geometric variation on width and shift in frequency of band gaps and comparing the two models in order to find a compromised one for vibration control.

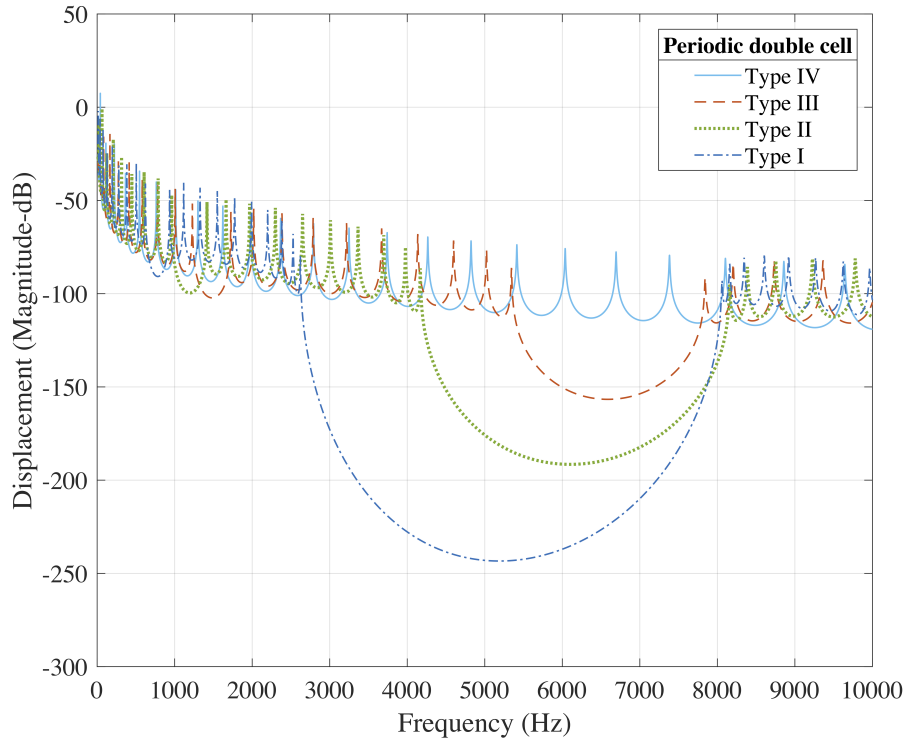


Figure 10: WFEM frequency response function of periodic double cell beam for flexural waves

The application is based on flexural and longitudinal waves of perfectly periodic

models in Fig.10 and Fig.11. The analysis is applied for four types of geometrical variations as a test cases.

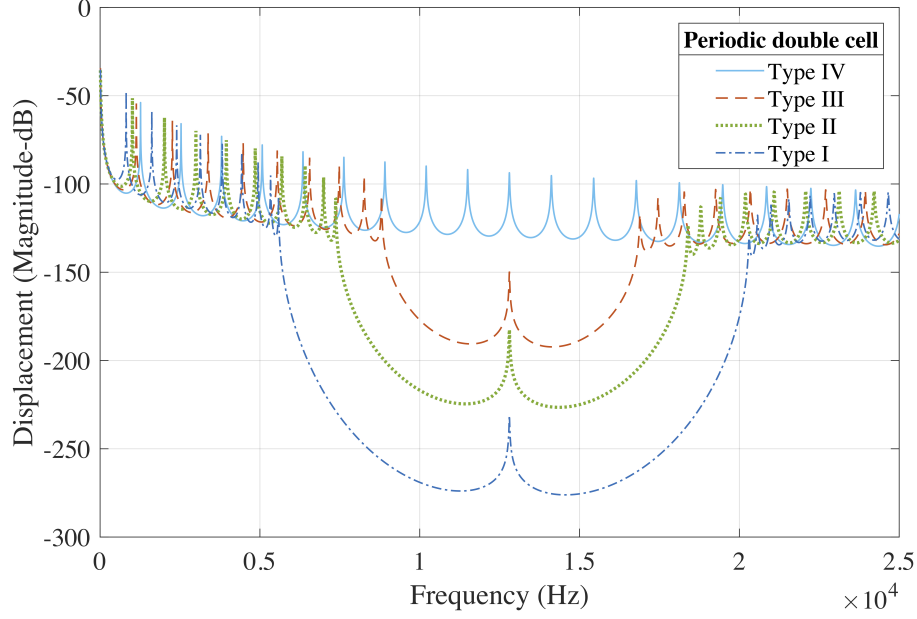


Figure 11: WFEM frequency response function of periodic double cell beam for longitudinal waves

Both, flexural and longitudinal waves are investigated under FB periodicity condition. The ranges of frequency of FRF of flexural waves in Fig.9 is considered at around 10 kHz, whereas for longitudinal waves in Fig.11 is around 25 kHz, depending on the frequency stop bands zone. More details on geometrical variation of the Types plotted in Fig.10 and Fig.11 are reported in Table 3. The response shows an enlargement in frequency stop bands as the height of cross section (B) decreases and the frequency stop bands tends to increase from almost 8 kHz up to around 2.5 kHz. Similarly, a frequency response function of the same periodic double cell is considered for longitudinal waves to describe the dynamic behaviour of beam in compression conditions.

Fig.11 shows an enlargement of frequency stop bands into the left and right sides of the frequency ranges. The result shows an enlargement of frequency stop bands compared to continuous beam type IV, characterised by no ranges of free wave propagation, to almost 15kHz range covered by stop bands.

Now we consider a super unit cell. In Fig.12 the frequency response function is derived in the frequency range $[0 - 1]$ kHz. The results are based on frequency band gaps shift and enlargement of width of the band gaps. Fig.12 shows a

frequency response function of a 6th order beam. It can be noted that band gaps move to higher frequencies at increasing the height of the second cell (B). For instance, the first subplot which is dedicated for Type I (B height=15.36 mm) has a band gaps around 400 – 650 Hz. In case of Type II (B height=20.00 mm) the band gap is shifted to higher frequencies.

Ultimately, the use of super unit cell has a significant pros compared to the double unit cell. The first point that can be noticed in the FRFs of the Fig.12 is that there is a tremendous shift of frequency stop bands from lower to higher frequency ranges. The second point is that there is a frequency stop band appearing in lower frequency ranges bellow 1 kHz, which is not the case in double unit cell approach. In conclusion the characteristics of the beam with Fibonacci series or simply (quasi-periodic beams) is that the geometrical impedance mismatch between the non-symmetrical interfaces in these types of beams gives an efficient impact on reducing the response especially in lower frequency regimes compared to (ABABABABABABA) periodic case. If we consider in terms of band gaps, it does not show an efficient result in creating wider stop bands, but it has multiple attenuation level in lower and medium frequency ranges. The results obtained in this paper shows that the beam with Fibonacci characteristics can improve performances in terms of attenuation level without weight penalty, which can be an asset for meta-materials.

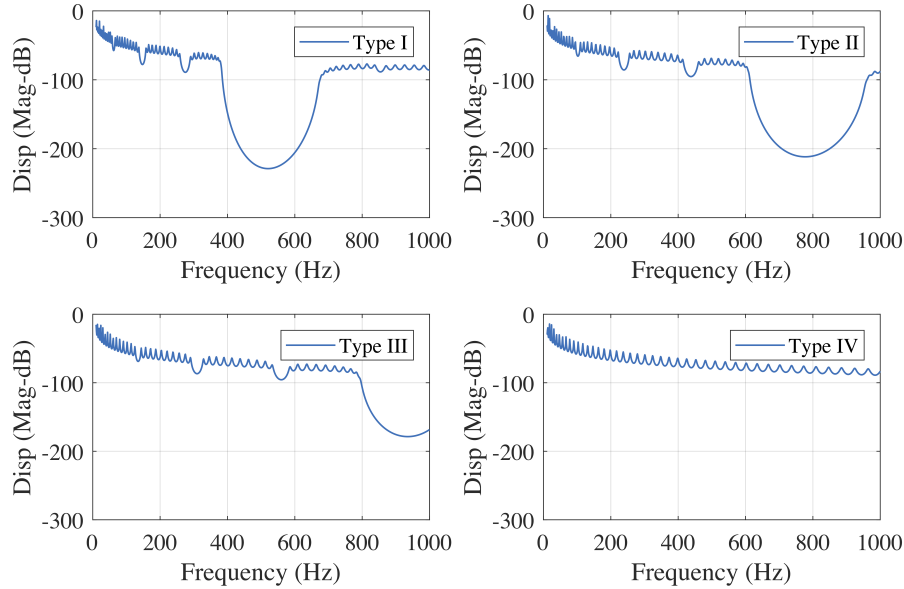


Figure 12: WFEM FRF for flexural waves of super unit cell with 6th order of Fibonacci sequence

4.3 Frequency response function of quasi-periodic beam with geometrical variations of type *II*:

This test case is influenced by the previous results. As it can be seen from Fig. 10, Fig. 11 and Fig. 12, that there is an evident band gaps shift and width enlargement while the factor of the cross sections of Tab.3 increased from (1 – 2.7). Now in this sub-section the same procedure is applied to the quasi-periodic beam with the 11th order of Fibonacci using four types of geometrical variation according to the Tab.3. Fig.13 shows four curves, each corresponding to the four cross-section types of variations. Type *IV* is a continuous beam without impedance mismatch of the cross-section, while the others include geometrical variations. Starting from Type *III* with dashed line, Type *II* dot curve line, and Type *I* with dot dashed line, each has stop bands in different ranges of frequencies. It can be highlighted that by increasing the factor of the geometrical variation the wide of band gaps is increasing. There are some few band gaps that exist in Type *II* and *III* but not as deep as Type *I*.

In conclusion, case M1 shows significant impacts on vibration control of the

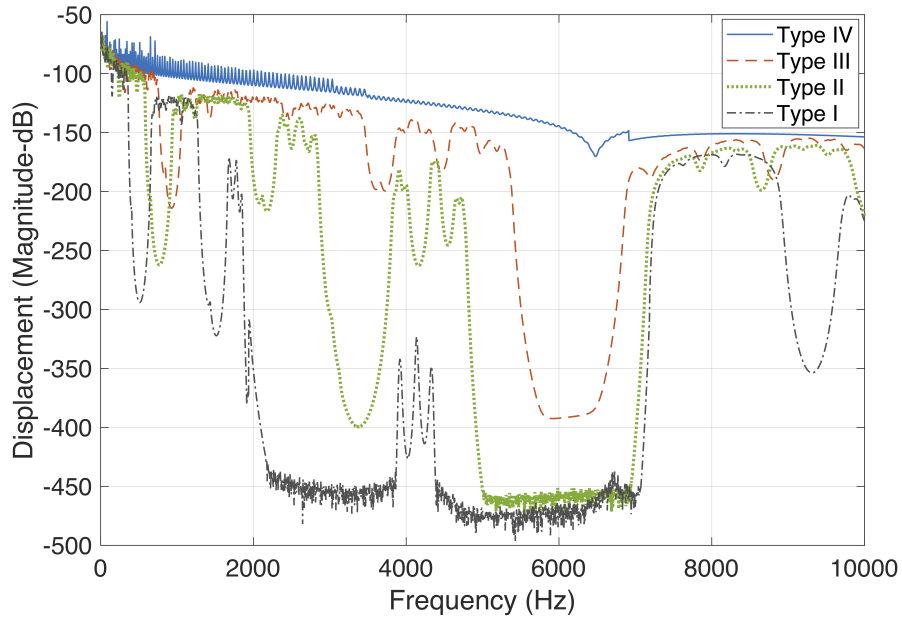


Figure 13: FRFs of the flexural waves for 11th order of Fibonacci beam with geometrical variation

beam span. The first case, flexural analysis shows that, by increasing the length of Fibonacci orders, the depth of the band gaps grows deeper and it is also emphasised in longitudinal waves. The second part describes width enlargement and shift in frequency of band gaps, in which quasi-periodic super unit cell shows

more impact compared to the double unit cell approach.

4.4 FRF results for Case M2

The second quasi-periodicity configuration is based on the impedance mismatch of material constituents. The beam is analysed as a continuous span (with no cross section variation). The mass of the system for all orders of Fibonacci is kept the same, while the length of the beam is changed and the number of cells are increased according to Fibonacci pattern. the length of the structure varies from 0.5 m to 14.4 m that includes [4th, 5th, 6th, 7th, 8th, 9th, 10th, 11th] orders of Fibonacci with [5, 8, 13, 21, 34, 55, 89, 144] cells. The results of the dynamic analysis for flexural waves in Fig.14 shows similar behaviour as those for the geometrical impedance mismatch in terms of increase of the depth of the band gaps when the order increases.

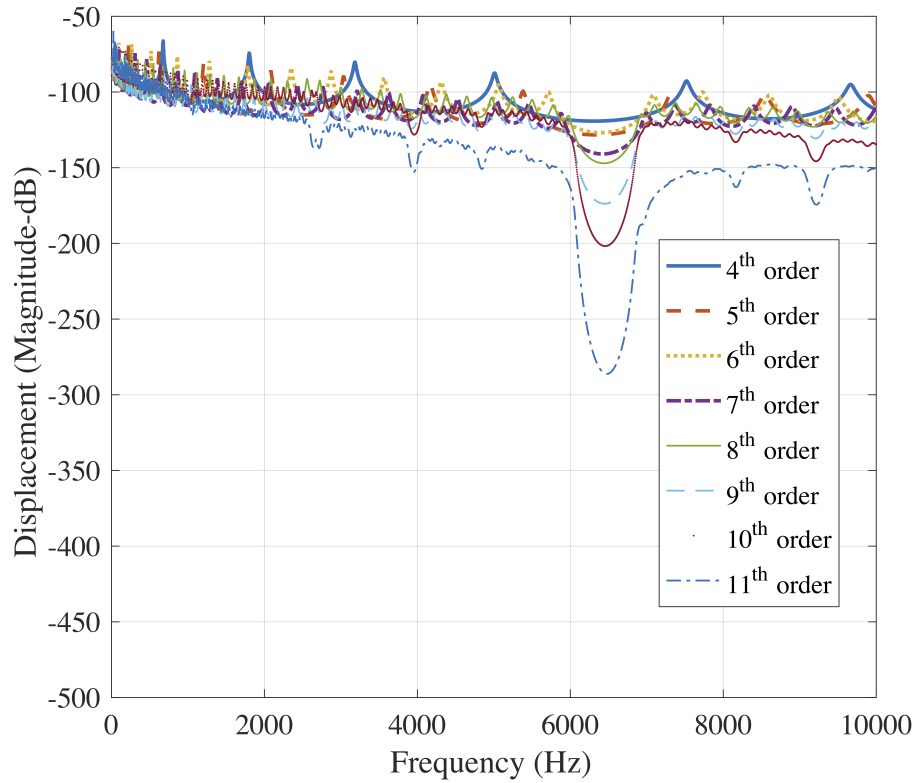


Figure 14: FRFs of the flexural waves for given orders of Fibonacci beam with material variation.

The main result in this analysis is that material constituent discontinuity does

not have a high dynamical influence in the depth growth of frequency stop bands as it is in the cross section variation case. Analysing again the numerical results in comparative way (i.e. without paying attention to the absolute values), the growth of depths in the frequency band gaps is lower than those computed for the variation of cross-sections.

Fig. 15 is dedicated to the longitudinal waves of the case $M2$, where it shows a change in the location of band gaps compared to the flexural waves. The ranges of band gaps can be observed in two locations between $[4400 - 4800]$ Hz and $[6700 - 10000]$ Hz. It has much better influences regarding the locations of the band gaps compared to the flexural waves and also the depth is gradually becoming larger.

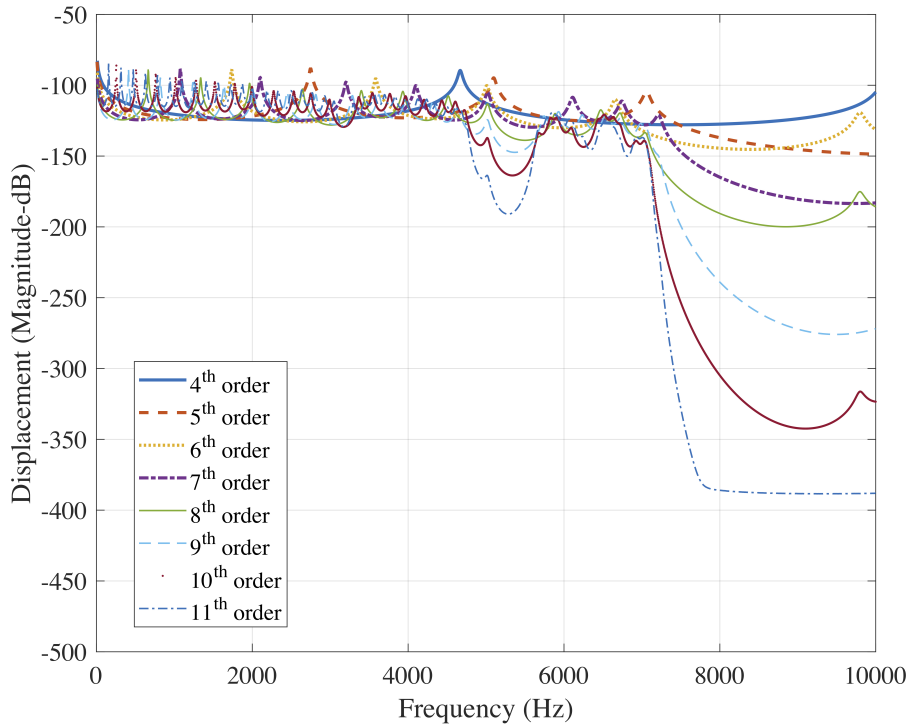


Figure 15: FRFs of the longitudinal waves for given orders of Fibonacci beam with material variation.

The response of the 11th order of Fibonacci beam in the FRF shows a flat curve in the larger band gaps location (without any higher dynamics), that is due to the longer length of the beam. Beside the flexural and longitudinal (FRFs) of the case $M2$, another extra sub-case scenario has been investigated by considering combination of lower and higher sound velocity materials. As there was not

a big difference between the sound velocity of (Aluminium 2045-T4) and (Steel A-36), two other materials (copper and magnesium) are also taken into account for the flexural FRFs of the 11th order of Fibonacci sequence.

Fig.16 shows three curves, each corresponding to the material combination of case M2. Steel A-36 is selected as a constant material (cross-section (A)) and the copper, aluminium and magnesium are varied according to the Fibonacci sequence alongside axial direction as (cross-section (B)). The results shows that materials combination of steel and copper respectively with velocity of $5063m/s$ and $3503m/s$ has a very low depth of attenuation and narrower band gaps marked in solid line in the frequency ranges between $[5000 - 7000]$ Hz. In contrary materials combination of steel with aluminium and magnesium respectively with velocity of $5199m/s$ and $5042m/s$ are reported in dashed and dot dashed lines which has larger depth and wider band gaps compared to the copper one.

In conclusion, the dynamic response of quasi-periodic finite span reduces while

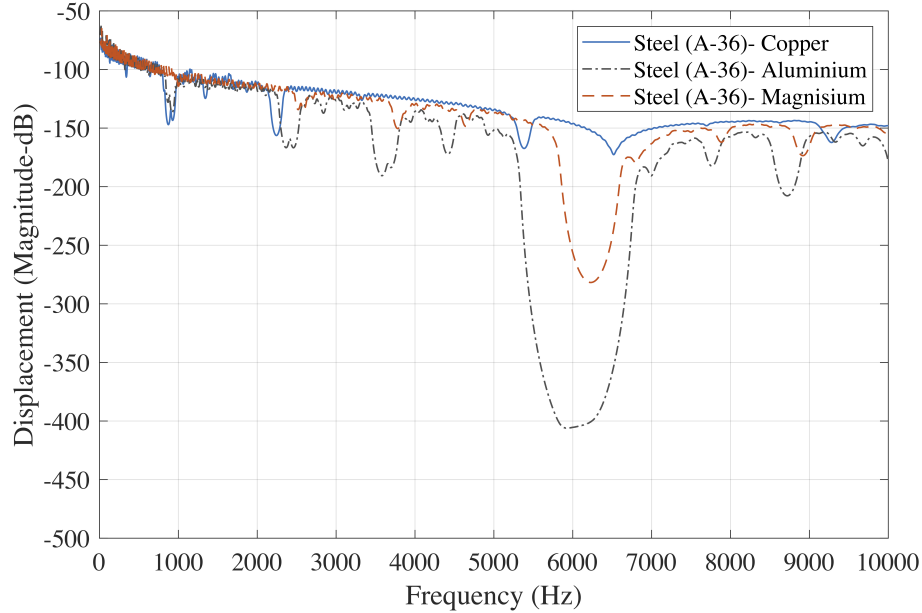


Figure 16: FRFs of the 11th order of Fibonacci beam with material variation.

keeping the four types of variations. It seems from the lexicon that the sound velocity of case M2 with constant cross sections and material variation is simply the ratio between modulus of elasticity and density. In contrary, the sound velocity of case M1 with constant material and cross section variation is the ratio of modulus of elasticity with respect to density multiplied by a factor that is squared of height of the cross section. Thus, it explains that M2 is less efficient

in terms of change in the impedance mismatch.

5 Spectral analysis of the M1 waveguides

5.1 Double cell

The same transfer matrix, extracted for the FRFs of the previous results based on periodic double cell, is used again for dispersion curves computation. Frequency-shift of the stop/pass band positions is quantified, using the real solution of waves [41]. Herein, for quantifying the frequency shift of stop bands, the dispersion curves are plotted considering only the real parts of propagative waves. In Fig.17, three types of cross-section variation for double cell periodicity is plotted by fixing type *I*. The investigated frequency range is zoomed to $[0 - 2]$ kHz for periodic double cell in order to visualise precisely the shift of band gaps. There is one main observation: the shift in frequency. Concerning the first, again the band gaps move to higher frequencies at increasing the height of cross section B. The frequency stop bands in the first types is around $[650 - 850]$ Hz, whereas for Type *II* it shifts to higher frequencies at around $[1000 - 1350]$ Hz with a little width compared to first type.

In Type *III*, band gap moves to higher frequencies $[1300 - 1600]$ Hz. Evaluating the stop band width in four cases, it seems that the stop band width is enlarging after Type *I* up to Type *III*, while in Type *IV*, the width of stop band tends to disappear with a shift to higher frequencies compared to the other types. In fact, it gradually shifts by reducing the height of the second cross section (B) as it reaches the zero impedance mismatch in Type *IV*.

5.2 Super unit cell

Similarly, an important part of analysis had to be taken into account for the spectral analysis of the quasi-periodic embedded super unit cell in periodic infinite systems. Fig.18 shows the dispersion curves of 6^{th} order of Fibonacci. The same technique used for the dispersion of fully periodic double cell is also considered in this system. Again the comparison is plotted between Type I, used as reference, and the other Types.

Comparing the results, in terms of real part of the wave number, of periodic beam Fig.17 and quasi-periodic beam Fig.18 it can be noted that in both cases the stop bands shift to higher frequencies but for the quasi periodic beam it changes quite dramatically. In fact, comparing the same band gap for the two beams it can be noted that the band gap in quasi-periodic beam is almost 2 times larger than periodic one. In view to be more clear in Fig.19 a comparison between band gaps of periodic and quasi periodic beam, at same cross section ratio, is provided. The horizontal axis of the plot shows an average

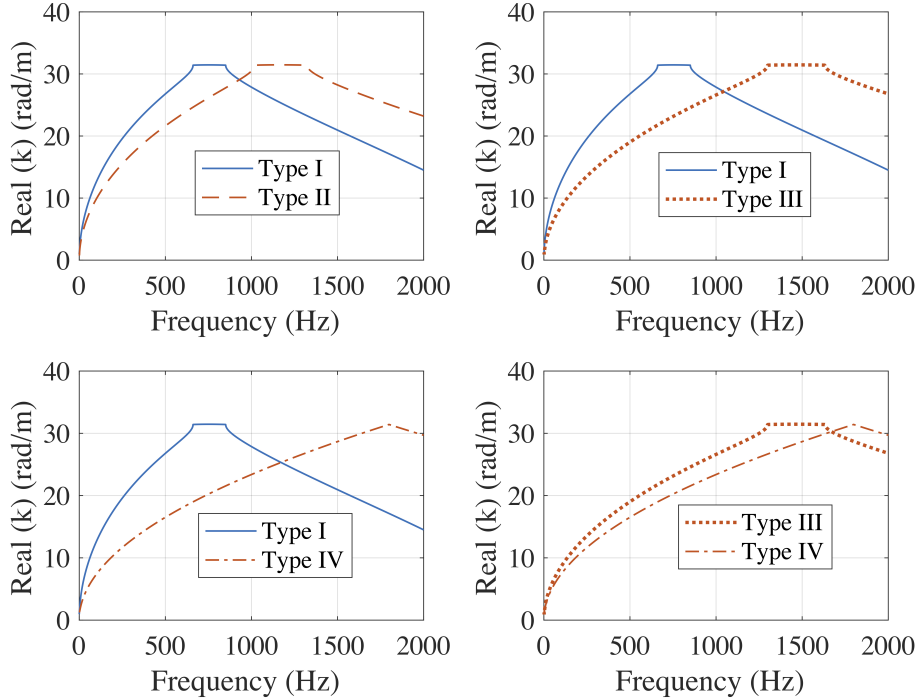


Figure 17: WFEM frequency response function of periodic double cell beam for flexural waves

frequency which corresponds to the band gaps interval Δf over the overall selected range of frequency f in each Fig.17 and Fig.18 respectively. The plot has two different curves, the blue one corresponds to the fully periodic beam with double cell including the geometrical cross-section variation, whereas the red curve corresponds to the quasi-periodic beam with the 6th order of Fibonacci and including those four types of geometrical cross section variation effects. The band gap width of quasi periodic beam is higher then the periodic one up to ratio 2. After that the band gap width of periodic increases by increasing the ratio, while the band gap of quasi periodic decreases.

6 Comparison of two quasi-periodic models (Fibonacci & Thue-Morse)

In this section a comparison of flexural waves obtained by investigating two different quasi-periodic models, Fibonacci and Thue-Morse sequence [22], is discussed. The Thue-Morse sequence can be obtained within the present approach always invoking the [A] and [B] base modules. In view to compare beams hav-

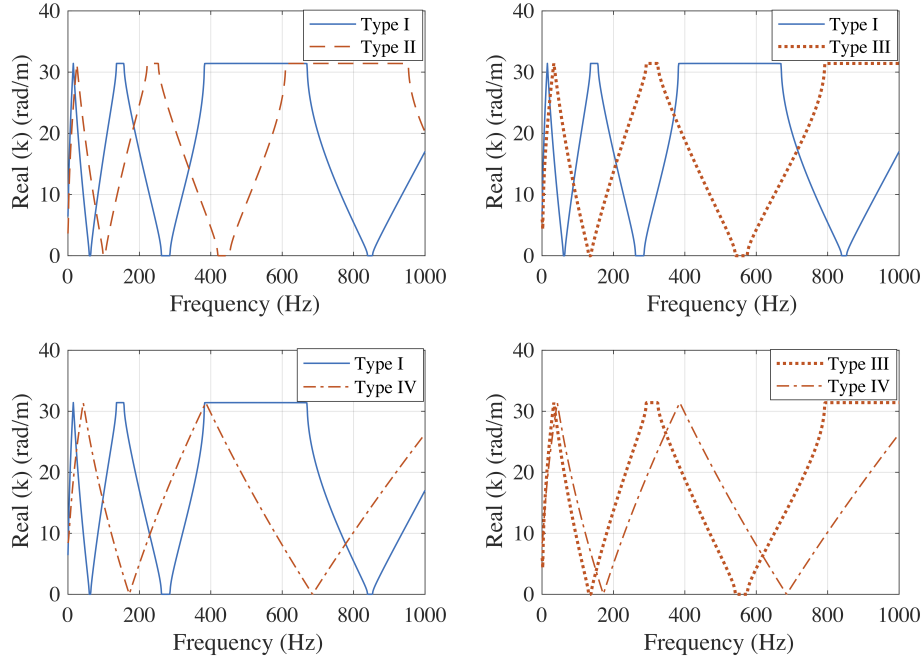


Figure 18: Dispersion curve of super unit cell with 6^{th} order of Fibonacci sequence

ing the same mass, since the two models follow different sequences, the two models have two different orders: 5^{th} for Fibonacci and 3^{rd} for Thue-Morse. For the Fibonacci case the beam is composed of 8 unit cells with the sequence [ABAABABA], Fig.1: whilst for the Thue-Morse case the beam consists of 8 cells following this sequence [ABBABAAB]. Hence, the beams have constant masses and same length but with different material properties. Cell(A) is made of steel ($A-36$) whereas cell(B) is made of Aluminium alloy ($2045-T4$). There are 8 unit cells in each beam. The length of the beam is 80 mm. They have free-free boundary conditions and are forced with a unit spectrum force in the first node while the response is taken from the last node of the beams.

Comparison is made by comparing FRFs and spectral analysis and results are reported respectively in Figs.20 and 21. The results carried out from the two models are both good showing different levels of attenuation with some differences in frequencies. In fact, focusing on the FRF results plotted in Fig.20, both the curves show a large stop band around [7800 – 9800] Hz with Fibonacci –10 dB lower attenuation level compared to Thue-Morse, but, in the remaining frequency range, there is another stop bands (less in width and depth) that appear in a frequency range for one model and in another frequency range for

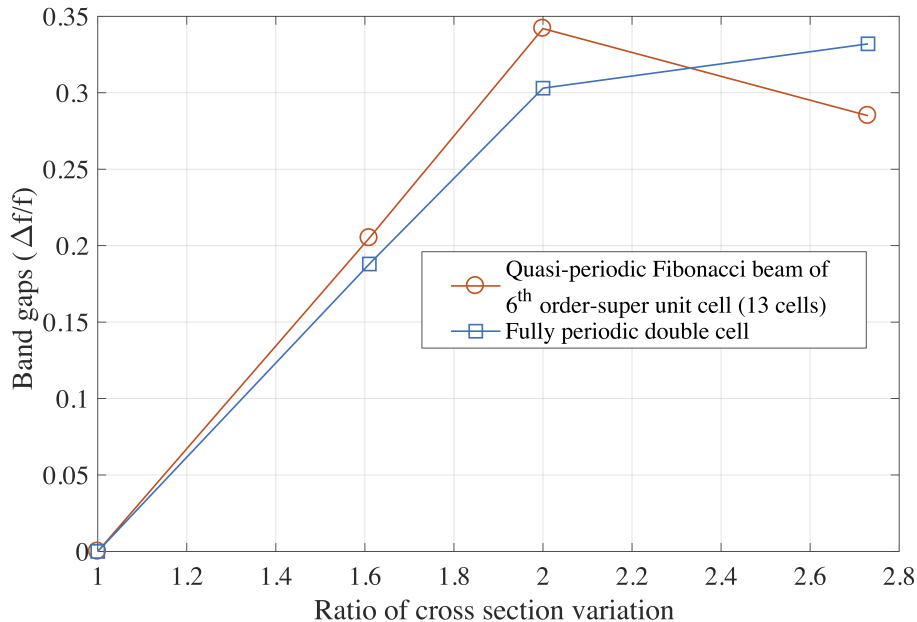


Figure 19: Spectral behaviour of band gaps for periodic and quasi-periodic embedded beams

the other one.

This is more evident in Fig.21 where the real and imaginary parts of the wavenumber are plotted. This plot is much visible and it can be noted that the number of stop bands for both curves are the same, but the width and the depth of the bands gaps for Fibonacci and Thue-Morse models is different. For instance in the frequency [2000 – 2500] Hz the stop bands of the Thue-Morse model outperforms, both in width and in depth, the one obtained by Fibonacci one. In the frequency range [3000 – 4000] Hz the behaviour is vice versa.

By accomplishing the outcome results of two different quasi-periodic models, it should be noticed that globally, both models perform similar results with a slight different width and the attenuation level. Fibonacci model has lower attenuation level in their large stop bands, which can lead to a compromised model in vibration control of beam spans.

7 Conclusions

The structural response of periodic and quasi-periodic beams are investigated. These beams are modelled using deterministic approach. Periodic beams are made of two different cells in terms of mass and cross section dimensions. Whereas quasi-periodic beams has the same configuration of cells made of these

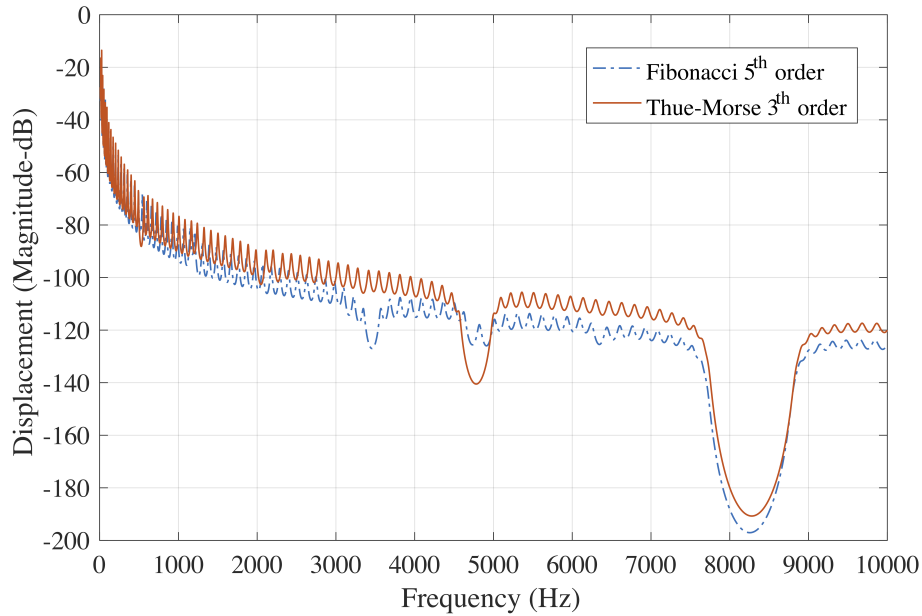


Figure 20: FRFs of the Fibonacci and Thue-Morse beams with the material variations.

two different cells but the replication of periodic cells are not perfect and it follows Fibonacci sequence pattern.

In the first case an analysis of the harmonic response of quasi-periodic beams with increasing orders (length) of Fibonacci sequence with the finite element method is investigated. In this case, beams are made up of cells (constant length) whose cross-section areas and materials properties follow a Fibonacci sequence is studied.

The second one relays on the four types of geometrical variations. The geometrical variations of case M1 are applied in the periodic and quasi-periodic beams of double and super unit cells. In this case while comparing the results, global mass of the beams are kept constant and cross sections are varied.

The last case consist of spectral analysis or the wave propagation behaviour of periodic structures with the WFEM. In this case beams are made up of identical super-unit-cells/patterns which are composed of cells whose properties follow Fibonacci sequence of a 6^{th} order.

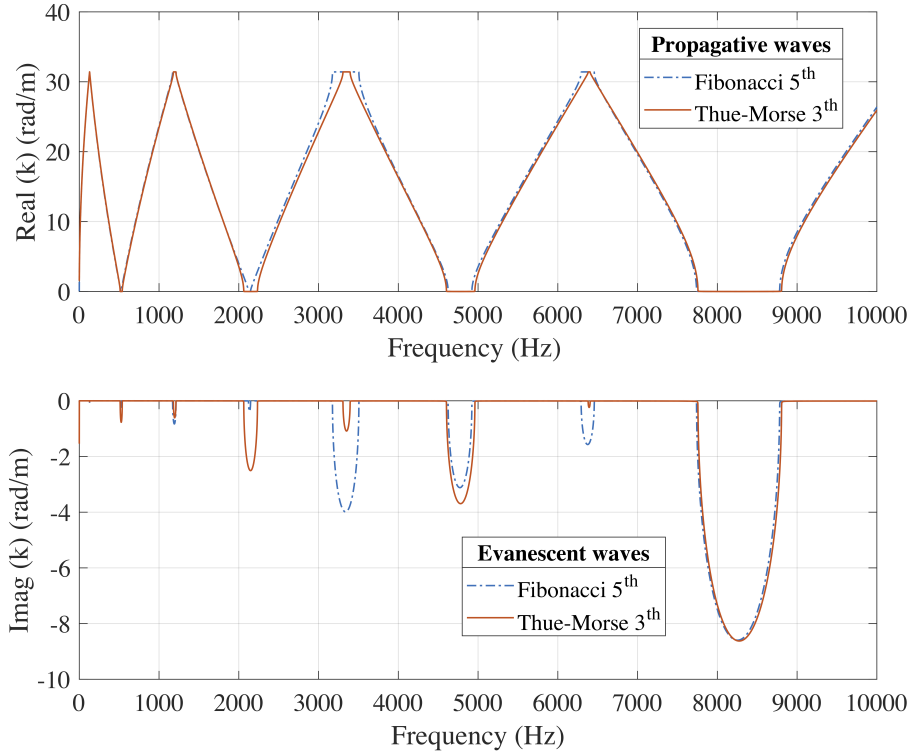


Figure 21: Dispersion curve of the Fibonacci and Thue-Morse beam based on flexural waves.

7.1 Main results

The first results by increasing the orders of a quasi-periodic beam with the impedance mismatch due to geometric variation (cross-section variation) give a clear view of the phenomena. A rapid growth in the depth amplitude of the band gaps by increasing the Fibonacci orders can be noted.

Studies of the geometric variation applied to a quasi periodic beam is extended, in a proper way for the periodicity condition, in the WFEM method to reduce and increase the volume representative of cross-section (A) and cross-section (B) proportionally, while keeping the total mass of the both cells constant. Focused on flexural and longitudinal waves, four types of numerical models are designed for the spectral analysis.

As stated in the last case study conclusion, a quasi-periodic beam with 6th order of Fibonacci sequence is placed in a super unit cell for FB waves analysis. Four types of cross-section variations in the beams are considered. The main results,

obtained for 6th order, show that a larger difference between the cross-sections (i.e. cross section (A) is much larger and cross section (B) is much smaller) lead to three main effects: i) change in extension/enlargement of frequency band gaps, ii) shift of frequency band gaps to lower frequency range and iii) an increase in the depth of amplitude of frequency band gaps.

Overall the quasi-periodic structures with geometrical impedance mismatch have an efficient impact on reducing the response in lower frequency regimes compared to strictly periodic counterparts. Although, it does not show large widths in lower frequency stop bands, but a small degree of geometrical impedance change, can shift the stop bands drastically compared to the strictly periodic spans. The results obtained have also shown that the quasi-periodicity can improve performance since attenuation, in given frequency range, can be obtained without weight penalty, which can be an asset for lightweight structures.

Highlights and contribution of the study

1. Forced response of quasi-periodic beams with increasing the order of Fibonacci, shows rapid growth in the depth displacement amplitude of the band gaps.
2. Forced response studies of four types of geometrical variations in identical super-unit-cells and double unit cells/patterns shows three aspects: i) change in extension/enlargement of frequency band gaps, ii) shift of frequency band gaps to lower frequency range and iii) an increase in the depth of amplitude of frequency band gaps.
3. Frequency response function of a quasi-periodic beam of 11th order with four types of geometrical and material variations gives an efficient results containing enlarging the wide of band gaps towards left and right of frequency ranges. For instance geometrical variation of *Type I* and material variation of (Steel-Aluminum).
4. Spectral analysis of four types of geometrical variations in identical super-unit-cells and double unit cells/patterns are analysed. The significant of periodic beam composed of cells whose properties follow Fibonacci sequence of a 6th order and cells whose properties follow a perfect periodic orders are studied. The results shows larger (Δf) for a unit cell with composition of cells following Fibonacci sequence.

Acknowledgements

This paper containing research investigation, carried out in the framework of the VIPER project (Vibroacoustic of PERiodic media). This project has received funding from the European Union's Horizon 2020 research and innovation program under Marie Curie grant agreement No 675441 and EUR EIPHI (ANR 17-EURE-0002) project.

References

- [1] K. F. Graff. *Wave Motion in Elastic Solids*. Dover Publications, 1975.
- [2] L. Cremer, M. Heckl, and B. A. T. Petersson. *Structure-Borne Sound: Structural Vibrations and Sound Radiation at Audio Frequencies*. Springer-Verlag, 3rd edition, 2005.
- [3] R. A. Di Taranto. Theory of vibratory bending for elastic and viscoelastic layered finite-length beams. *Journal of Applied Mechanics*, 32(4), 1965.
- [4] D. J. Mead and S. Markus. The forced vibration of a three-layer, damped sandwich beam with arbitrary boundary conditions. *Journal of Sound and Vibration*, 10(2):163—175, 1969.
- [5] V. S. Sokolinsky and S. R. Nutt. Consistent higher-order dynamic equations for soft-core sandwich beams. *AIAA Journal*, 42(2):374—382, 2004.
- [6] G. Kurtze and B. G. Watters. New wall design for high transmission loss or high damping. *The Journal of the Acoustical Society of America*, 31(6):739—748, 1959.
- [7] J. A. Moore. Sound transmission loss characteristics of three layer composite wall constructions. PhD Thesis, Department of Mechanical Engineering, Massachusetts Institute of Technology, Cambridge, Massachusetts (USA), May 1975.
- [8] C. L. Dym and M. A. Lang. Transmission of sound through sandwich panels. *The Journal of the Acoustical Society of America*, 56(5), 1974.
- [9] C. L. Dym and D. C. Lang. Transmission loss of damped asymmetric sandwich panels with orthotropic cores. *Journal of Sound and Vibration*, 88(3):299—319, 1983.
- [10] A. C. Nilsson. Wave propagation in and sound transmission through sandwich plates. *Journal of Sound and Vibration*, 138(1):73—94, 1990.
- [11] J. N. Reddy. *Mechanics of Laminated Composite Plates and Shells: Theory and Analysis*. CRC Mechanical Engineering Series. Taylor and Francis, 2nd edition, 2003.
- [12] S. Ghinet, N. Atalla, and H. Osman. The transmission loss of curved laminates and sandwich composite panels. *The Journal of the Acoustical Society of America*, 118(2), 2005.
- [13] R. Kumar and R. W. B. Stephens. Dispersion of flexural waves in circular cylindrical shells. *Proceedings of the Royal Society of London. A. Mathematical and Physical Sciences*, 329(1578):283-297, 1972.

- [14] C. R. Fuller. The effects of wall discontinuities on the propagation of flexural waves in cylindrical shells. *Journal of Sound and Vibration*, 75(2):207—228, 1981.
- [15] D. G. Karczub. Expressions for direct evaluation of wave number in cylindrical shell vibration studies using the Flugge equations of motion. *The Journal of the Acoustical Society of America*, 119(6), 2006.
- [16] J. R. Banerjee. Development of an exact dynamic stiffness matrix for free vibration analysis of a twisted Timoshenko beam. *Journal of Sound and Vibration*, 270(1—2):379—401, 2004.
- [17] Brillouin, L., 2003. *Wave propagation in periodic structures: electric filters and crystal lattices*. Courier Corporation.
- [18] Collet, M., Ouisse, M., Ruzzene, M. and Ichchou, M.N., 2011. Floquet—Bloch decomposition for the computation of dispersion of two-dimensional periodic, damped mechanical systems. *International Journal of Solids and Structures*, 48(20), pp.2837-2848.
- [19] Mead, D.J., 1973. A general theory of harmonic wave propagation in linear periodic systems with multiple coupling. *Journal of Sound and Vibration*, 27(2), pp.235-260.
- [20] Billon, K., Zampetakis, I., Scarpa, F., Ouisse, M., Sadoulet-Reboul, E., Collet, M., Perriman, A. and Hetherington, A., 2017. Mechanics and band gaps in hierarchical auxetic rectangular perforated composite metamaterials. *Composite Structures*, 160, pp.1042-1050.
- [21] Spadoni, A., Gonella, S., Ruzzene, M. and Scarpa, F., 2007, September. Wave propagation and band-gap characteristics of chiral lattices. In *ASME 2007 International Design Engineering Technical Conferences and Computers and Information in Engineering Conference September* (pp. 4-7).
- [22] Velasco, V.R. and Zarate, J.E., 2001. Elastic waves in quasiperiodic structures. *Progress in Surface Science*, 67(1-8), pp.383-402.
- [23] Shechtman, D., Blech, I., Gratias, D., and Cahn, J. W., "Metallic phase with long-range orientational order and no translational symmetry," *Physical review letters* 53(20), 1951 (1984).
- [24] Bindi, L., Steinhardt, P. J., Yao, N., and Lu, P. J., "Natural quasicrystals," *science* 324(5932), 1306-1309(2009).
- [25] Vardeny, Z. V., Nahata, A., and Agrawal, A., "Optics of photonic quasicrystals," *Nature Photonics* 7(3),177-187 (2013).
- [26] Kraus, Y. E. and Zilberberg, O., "Quasiperiodicity and topology transcend dimensions," *Nature Physics* 12, 624-626 (7 2016).

- [27] Kraus, Y. E., Lahini, Y., Ringel, Z., Verbin, M., and Zilberberg, O., Topological states and adiabatic pumping in quasicrystals," *Phys. Rev. Lett.* 109, 106402 (Sep 2012).
- [28] Ozawa, T., Price, H. M., Goldman, N., Zilberberg, O., and Carusotto, I., Synthetic dimensions in integrated photonics: From optical isolation to four-dimensional quantum hall physics," *Physical Review A* 93(4), 043827 (2016).
- [29] Kraus, Y. E., Ringel, Z., and Zilberberg, O., 4-dimensional quantum hall effect in a two-dimensional quasicrystal, *Physical review letters* 111(22), 226401 (2013).
- [30] Fikar, Jan (2003). Al-Cu-Fe quasicrystalline coatings and composites studied by mechanical spectroscopy. Ecole polytechnique federale de Lausanne EPFL, Thesis n 2707 (2002).
- [31] Kalman, Matthew (12 October 2011). "The Quasicrystal Laureate". MIT Technology Review. Retrieved 12 February 2016.
- [32] Jean-Marie Dubois, Song Seng Kang, Alain Perrot, Towards applications of quasicrystals, *Materials Science and Engineering: A*, Volumes 179-180, Part 1, 1994, Pages 122-126,
- [33] Suck, J.B., Schreiber, M. and Häussler, P. eds., 2013. *Quasicrystals: An introduction to structure, physical properties and applications* (Vol. 55). Springer Science & Business Media.
- [34] Hou, Z., Wu, F. and Liu, Y., 2004. Acoustic wave propagating in one-dimensional Fibonacci binary composite systems. *Physica B: Condensed Matter*, 344(1-4), pp.391-397.
- [35] Wu, Z., Li, F. and Zhang, C., 2018. Band-gap analysis of a novel lattice with a hierarchical periodicity using the spectral element method. *Journal of Sound and Vibration*, 421, pp.246-260.
- [36] Wu, Z.J. and Li, F.M., 2016. Spectral element method and its application in analysing the vibration band gap properties of two-dimensional square lattices. *Journal of Vibration and Control*, 22(3), pp.710-721.
- [37] Wu, Z.J., Li, F.M. and Zhang, C., 2015. Vibration band-gap properties of three-dimensional Kagome lattices using the spectral element method. *Journal of Sound and Vibration*, 341, pp.162-173.
- [38] H. Aynaou, E.H. El Boudouti, B. Djafari-Rouhani, A. Akjouj, V.R. Velasco Propagation and localization of acoustic waves in Fibonacci phononic circuits *J. Phys.: Condens. Matter*, 17 (2005), pp. 4245-4262
- [39] A.L. Chen, Y.S. Wang Study on band gaps of elastic waves propagating in one-dimensional disordered phononic crystals *Physica B*, 392 (2007), pp. 369-378

- [40] P.D.C. King, T.J. Cox Acoustic band gaps in periodically and quasiperiodically modulated waveguides. *J. Appl. Phys.*, 102 (2007), p. 014908
- [41] Gei, M., 2010. Wave propagation in quasiperiodic structures: stop/pass band distribution and prestress effects. *International Journal of Solids and Structures*, 47(22-23), pp.3067-3075.
- [42] Enrique Macia Barber. *Aperiodic Structures in Condensed Matter: Fundamentals and Applications*. CRC Press Published (2008), 432 pages.
- [43] Timorian, S., Franco, F., Ouisse, M., De Rosa, S. and Bouhaddi, N., 2018, September. Investigation for the analysis of the vibrations of quasi-periodic structures. *Proceedings of ISMA2018 International Conference on Noise and Vibration Engineering*, (pp.4551-4563).
- [44] Timorian, S., De Rosa, S., Franco, F., Ouisse, M. and Bouhaddi, N., 2019, July. Band diagram and forced response analysis of periodic and quasiperiodic panels. *Proceedings of 9th ECCOMAS Thematic Conference on Smart Structures and Materials*, (pp.1085-1095).
- [45] Becus, G.A., 1978. Wave propagation in imperfectly periodic structures: a random evolution approach. *Zeitschrift fur angewandte Mathematik und Physik ZAMP*, 29(2), pp.252-261.
- [46] Mester, S.S. and Benaroya, H., 1995. Periodic and near-periodic structures. *Shock and Vibration*, 2(1), pp.69-95.
- [47] Mencik, J.M. and Duhamel, D., 2016. A wave finite element-based approach for the modelling of periodic structures with local perturbations. *Finite Elements in Analysis and Design*, 121, pp.40-51.
- [48] Duhamel, D., Mace, B.R. and Brennan, M.J., 2006. Finite element analysis of the vibrations of waveguides and periodic structures. *Journal of sound and vibration*, 294(1-2), pp.205-220.
- [49] Pisano, L., 2002. *Fibonacci's Liber Abaci: A Translation into Modern English of the Book of Calculation, Sources and Studies in the History of Mathematics and Physical Sciences*, Sigler, Laurence E trans.
- [50] Nastran, M.S.C., 2004. *Quick reference guide. MSC. SOFTWARE*, 1.
- [51] Cook, R.D., Malkus, D.S. and Plesha, M.E., 1974. *Concepts and applications of finite element analysis (Vol. 4)*. New York: Wiley.
- [52] Arnold, L., Crauel, H. and Eckmann, J.P. eds., 2006. *Lyapunov exponents: proceedings of a conference held in Oberwolfach, May 28-June 2, 1990*. Springer.